

Morphology Development in Polypropylene/Polystyrene Blends During Coalescence Under Shear

Yun-Yan Li, Zi-Qi Chen, Yi Huang, Jing Sheng

School of Material Science and Engineering, Tianjin University, Tianjin 300072, China

Received 18 May 2006; accepted 4 November 2006

DOI 10.1002/app.25736

Published online in Wiley InterScience (www.interscience.wiley.com).

ABSTRACT: Morphology development during the coalescence under shear in polypropylene/polystyrene blends was studied in this article. The coalescence was performed by decreasing the shear rate after a fine morphology is obtained at higher shear rate. Time resolved SEM performance indicates that, because of the smaller capillary number, particles of the minor phase are almost spherical during the whole coalescence process. An original sizing method based on SEM is used to describe the time evolution of particle size and their distribution. Initially, the volume-average particle size increases rapidly and levels off before a steady state is obtained, while the number-average particle size increases

slowly but monotonously during the whole coalescence process. This two-step increase in volume average particle size is discussed in terms of coalescence efficiency. Further, an examination of scaling behavior shows that a master curve for particle growth with different compositions is observed by plotting the relative increase in particles size versus the shear strain, confirming that the evolution of particle size could be described by a scaling law. © 2007 Wiley Periodicals, Inc. *J Appl Polym Sci* 104: 666–671, 2007

Key words: polypropylene; polystyrene; coalescence; morphology

INTRODUCTION

In view of the significant effect of microstructure of blends on properties of final products, controlling the morphology development during blending is of importance. Studies concerning morphology development of polymer blends during mixing suggest that the final microstructure of blends is generally considered to be the result of a dynamic equilibrium between the breakup of particles and their coalescence. Therefore, obtaining a material with given properties requires a better understanding of the main mechanism governing the morphology development during mixing, that is, particle breakup and coalescence.

Research on the role of particle breakup in controlling phase morphology has a long-standing tradition. The inaugurator should be tracked back to Taylor¹ who studied quantitatively the breakup of single Newtonian particle in Newtonian matrix. Neglecting the coalescence between approaching particles, Taylor has given a model in terms of the interfacial tension and shear force to predict the final particle size. Studies along these lines was continued by Torza et al.,² Wu,³ and other researchers. Based on experimental data by

Grace,⁴ De Bruijn⁵ reported an empirical relation for the dependence of the critical particle size by breakup on shear rate.

When compared with particle breakup, coalescence, which still plays an important role in controlling the morphology development and final structure of blends to a great degree, was paid more attention until recent years. Early research on coalescence mainly focused on the coalescence in solvent-cast blends^{6–8} or melt blends under quiescent conditions.^{9–11} Unfortunately, the driving forces for the static coalescence are complicated by such factor as Brownian motion, van der Waals interactions, particles reshaping and so on, making it much different to study the general mechanism of coalescence in polymer blends; moreover, it is more considerate to regard the coalescence, which completes and cooperates with particle breakup to make a steady-state morphology during the mixing, as a flow-driven coalescence rather than the conventional static annealing. Consequently, studies regarding the coalescence during shear, that is, the flow-driven coalescence, are attracting more interest from both academic and commercial institutes. Theoretical studies on flow-driven coalescence involve mainly the establishment of numerical models to predict the variation of particle size as a function of coalescence time as well as mathematics behaviors (e.g. the scaling law) during coalescence. Smoluchowski¹² treated coalescence as an ideal collision process with particle interaction being neglected and suggested an unperfect model to characterize the main mechanism of coalescence. Subsequently, Zeichner and Schowalter¹³ im-

Correspondence to: J. Sheng (j_sheng@163.com).

Contract grant sponsor: Natural Science Foundation of China; contract grant number: 50390090.

proved this model by considering hydrodynamic interaction that is related to the trajectories of particles. Despite that this trajectories theory is relatively improved, it still could not give an accurate description about the coalescence especially between large particles on account of the ignoring of particle deformation. Considering particle deformation and squeezing flow of matrix, Chester¹⁴ made a different correction on Smoluchowski's theory, making it much effective to describe the flow-driven coalescence. Experimental study concerning the coalescence of particles in polymer blends is beginning to appear in the past few years.¹⁵⁻¹⁷ These studies make it more convenient to verify the aforementioned coalescence theories and improve these models further. Unfortunately, because of the difference in polymer systems studied in these works, some results (e.g., the shear rate dependence of coalescence dynamic and the morphology development after annealing) are contradict, indicating that the coalescence mechanism might depend greatly on the specific blending system, that is, the properties of each components of blends. Thus, it is meaningful to study further the driven-flow coalescence in another polymer blends different from those discussed earlier. In the present work, the morphology development during coalescence under shear was studied to probe how the size and distribution of particles of the minor phase change with time by the coalescence in the absence of breakup process. For this purpose, a polymer blend of polypropylene/polystyrene (PP/PS) was chosen to compare the coalescence behavior with that of Newtonian fluid.

EXPERIMENTAL

Materials

The basic materials used in this study were of commercial grade polypropylene (PP, 1300) with a density of 0.91 g/cm³, \bar{M}_w of 5.0×10^5 g/mol and a glass transition temperature of 17°C, and a commercial grade polystyrene (PS, 666D) with a density of 1.05 g/cm³, \bar{M}_w of 5.8×10^5 g/mol and a glass transition temperature of 111°C. All these materials were supplied by Beijing Yan-shan Petrochemical (Beijing, China).

Blends preparation

PP and PS were blended in a batch internal mixer with rotor diameter of 35 mm (XXS-300 torque rheometer produced by KeChuang Machinery, China). Prior to processing, all materials were dried for 12 h under vacuum at 80°C. To probe the size of the dispersed phase during the coalescence, a flow procedure corresponding to a two-step down in shear rate was applied: PP and PS were firstly mixed in different compositions at a higher shear rate of 96 S⁻¹ at 195°C for 10 min followed

by 50 S⁻¹ for 5 min to obtain a fine morphology. Subsequently, the shear rate was reduced to 1 S⁻¹ so as to induce coalescence. According to simultaneous studies processing in our lab, this lower shear rate of 1 S⁻¹ ensures that the subsequent morphology development was dominated by coalescence mechanism. To examine the morphology development during coalescence, samples at different coalescence time were taken out of the mixer and were immediately quenched in liquid nitrogen to freeze the original structure for the observation in a scanning electron microscope (SEM).

Morphological characterization

A SEM (Philips XL30) operated at an accelerating voltage of 20 kV was used to examine the fracture morphology of blends. The preblended samples were broken in liquid nitrogen and the fracture surface was covered with gold for the observation in the microscope (the thickness of the gold layer is about 20 nm). To make sure the original structure of blends intact, the surface was not etched.

The morphology was quantified using a self-made software. Contour and mass center of each particle were detected and each particle was scanned by straight lines going through the mass center from different directions, and the span from one side of a particle to the other, which is defined as the particle diameter d in this article, was noted by a computer; consequently, the average size of particles can be calculated by averaging the d values. Further, the maximum and minimum of the d can be easily obtained to describe the particle deformity, which will be discussed in the results. To obtain more reliable data, about 500 particles were considered to calculate these structure parameters for each micrograph. Further, two different average particle diameter, that is, the number average diameter d_n and the volume average diameter d_v were calculated based on eq. (1)

$$d_n = \frac{\sum_{i=1}^{\infty} n_i d_i}{\sum_{i=1}^{\infty} n_i} \quad d_v = \frac{\sum_{i=1}^{\infty} n_i d_i^4}{\sum_{i=1}^{\infty} n_i d_i^3} \quad (1)$$

RESULTS AND DISCUSSION

Figure 1 shows the SEM micrographs of PP/PS blends at different coalescence time. The blends have particle/matrix morphology with PP being the dispersed phase. These images show that the initial morphology consists of relatively small particles with a rather narrow size distribution. After 5.0 min, some approaching particles collide and coalesce while others could not find a partner for coalescence during this stage, which makes the size distribution relatively broader. This phenomenon is more pronounced as the coalescence proceeds. At

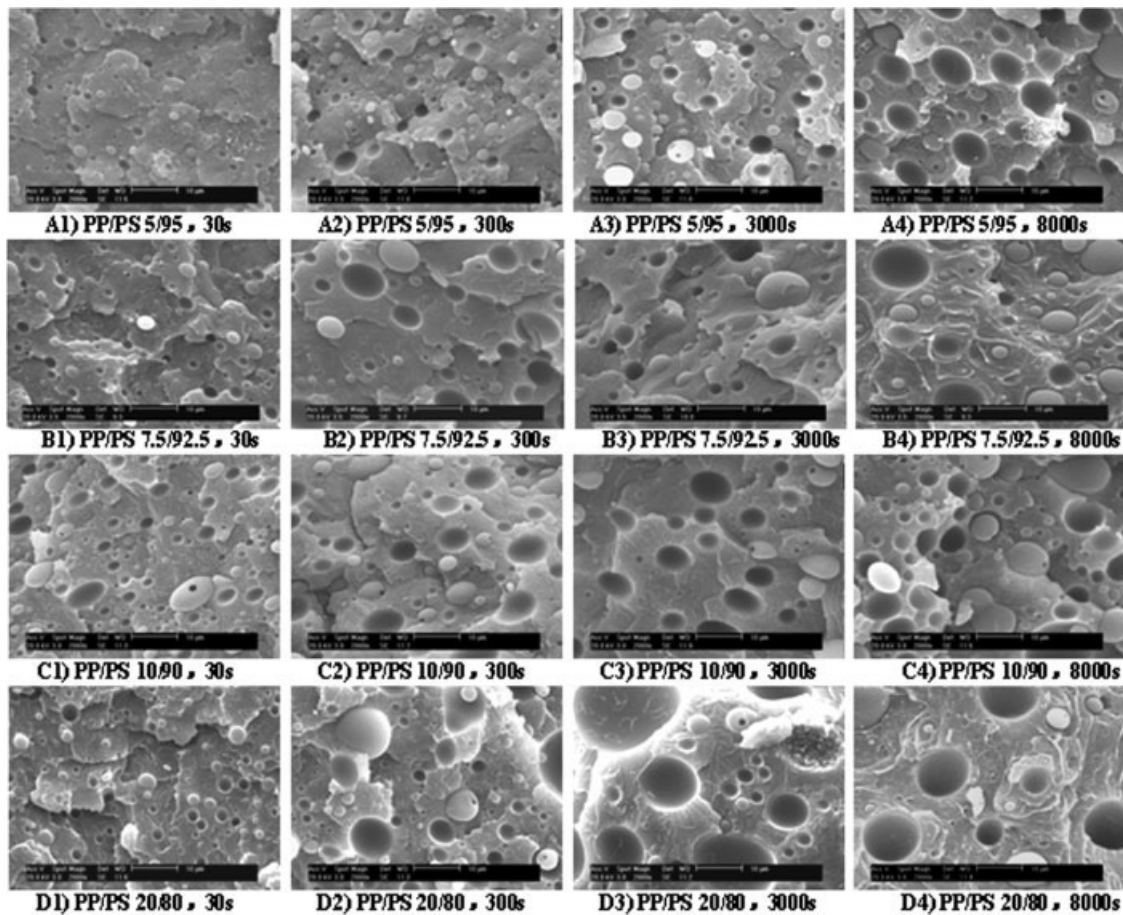


Figure 1 SEM and corresponding binary images of PP/PS blends at different coalescence time: A. PP/PS (5/95); B. PP/PS (7.5/92.5); C. PP/PS (10/90); D. PP/PS (20/80).

50 min, despite the appearance of very large particles, small particles whose size is comparative with that just after the beginning of coalescence still exist in blends, which indicate that the size distribution becomes more asymmetric. Because of the significant effect of phase dimensions on properties of blends, evolution of phase dimension and their distribution will be studied in detail in this article, but this will be discussed later. In respect of an unneglectable fact, that is, most particles remain spherical during the whole coalescence process, which is completely different with that during the process of particle breakup, the variation of particle shape will be firstly investigated in follows. For this purpose, the particle deformity^{1,18} defined as

$$D = \frac{d_{\max} - d_{\min}}{d_{\max} + d_{\min}} \quad (2)$$

is calculated and the typical variation of D as a function of shear strain (the product of coalescence time and shear rate) is shown in Figure 2. As can be seen, D fluctuates slightly around 0.08, indicating that no distinct particle deformation occurs during the whole coalescence process. This result can be explained roughly by means of the empirical relation between D and capillary number C_a suggested by Cox¹⁹ as well

as C_a defined by Taylor¹ in terms of the shear force and the interfacial tension.

$$D = \frac{5(19p + 16)}{4(p + 1)\sqrt{(20/c_a)^2 + (19p)^2}}, \quad C_a = \frac{\eta_m \dot{\gamma} d}{\sigma} \quad (3)$$

where p is the viscosity ratio, η_m is the viscosity of the matrix, $\dot{\gamma}$ is the shear rate, d is the particle diameter, and σ is the interfacial tension. For large reduction in shear rate, the particle produced by initially higher shear rate is sufficiently smaller than the minimum particle size determined by the critical capillary number $(C_a)_{\text{crit}}^1$ leading to a much smaller C_a than $(C_a)_{\text{crit}}$ and consequently, a negligible deformation. On the other hand, since particle breakup often occurs when $C_a > (C_a)_{\text{crit}}$ the smaller C_a makes it impossible for particle to breakup further at lower shear rate, which theoretically confirms that the morphology development is mainly controlled by coalescence mechanism to some extent.

Figure 3 represents the shear strain dependence of average particle size. To facilitate the analysis of size evolution at small shear strain, a logarithmic scale is used for the shear strain. From Figure 3, the number-average size increases slowly and monotonously while the volume

ED1

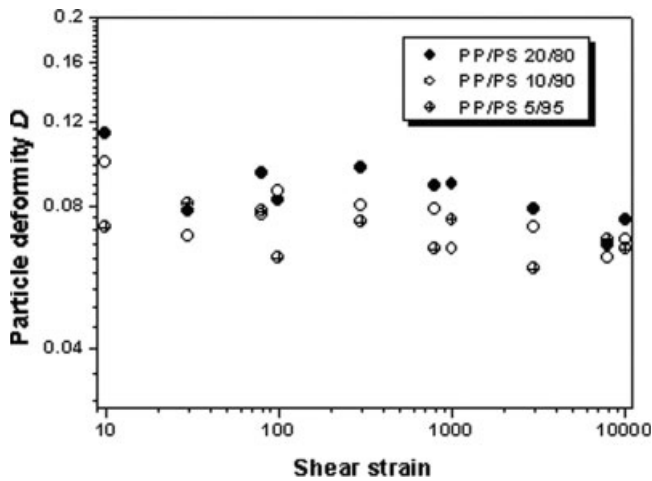


Figure 2 Evolution of particle deformity of PP in PP/PS blends with different compositions.

average size increases rapidly at the beginning of coalescence and levels off in a second step before a steady state size is reached. It should be noted that the time necessary to reach the final particle size is much longer than that investigated in this work; therefore, it is more appropriate to regard the measured final size as a pseudo steady state rather than a true steady state. However, in view, the coalescence rate in the last stage of coalescence is so small that this pseudo steady state is basically identical with the true one, the morphology development in the last stage will not be discussed in this study.

The two-step evolution in particle size has also been discussed experimentally before and can be interpreted by means of corresponding theory about shear-induced coalescence kinetics, that is, a coalescence model proposed by Swift and Friedlander.²⁰

$$\frac{dd(t)}{dt} = \frac{4}{\pi} (2 - 2^{\frac{2}{3}}) \phi_0 \dot{\gamma} d(t) E_0 \quad (4)$$

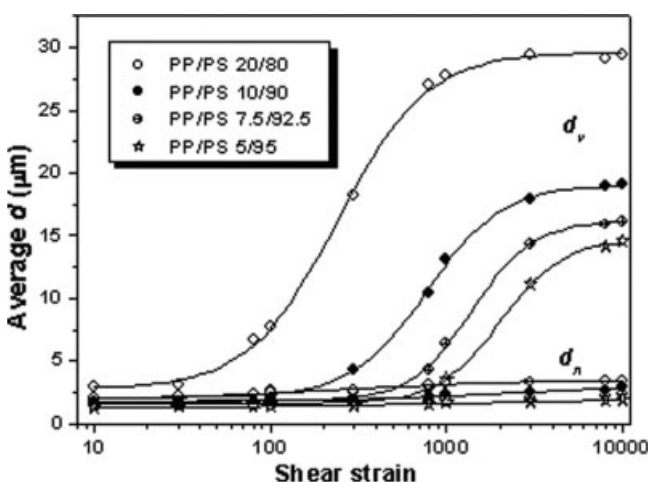


Figure 3 Shear-strain dependence of d during coalescence.

where ϕ_0 is the volume fraction of the minor phase and E_0 is the collision efficiency or equivalently, the coalescence efficiency which is essentially unaffected by deformation and equals to that of spherical particle²¹ for sufficiently small particles and decreases exponentially with the ratio of the predicted film-drainage and particle interaction times during collision when the particle size increases beyond a critical value d_{crit} , that is,

$$E_0 \propto \exp\left(-\frac{t_{drainage}}{t_{interaction}}\right) = \exp(-[md(t)]^{\frac{5}{2}} \dot{\gamma}^{\frac{3}{2}}),$$

$$m = 0.358 \left(\frac{p}{h_c}\right)^2 \left(\frac{\eta_m}{\sigma}\right)^{\frac{5}{2}} \quad (5)$$

where h_c is the critical thickness of the matrix film between approaching particles below which coalescence will occur immediately. Despite some assumption and restriction in this model, it is still effective to describe the coalescence behavior in viscoelastic polymer fluid.²² For coalescence in PP/PS blends, because of the small particle size at the beginning of coalescence, the coalescence efficiency or equivalently, the coalescence rate is higher, and consequently, a rapid increase in particle size appears. To the second stage, the increase in the film drainage time caused by the particle growth decreases the drainage probability and slows down the coalescence, making the particle size approach to a steady value.

On the other hand, to examine whether the particle size will increase exponentially shortly after the commencement of coalescence, which is theoretically tenable when particle size is smaller than d_{crit} as suggested by eq. (4), relation between particle size and shear strain is given in another form by using logarithmic scale to the particle size axis (Fig. 4). However, such linear relation

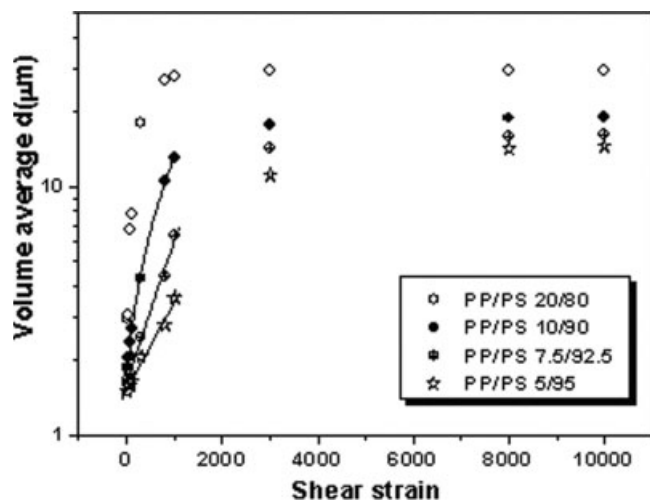


Figure 4 Strain dependence of d during coalescence in logarithmic coordinate.

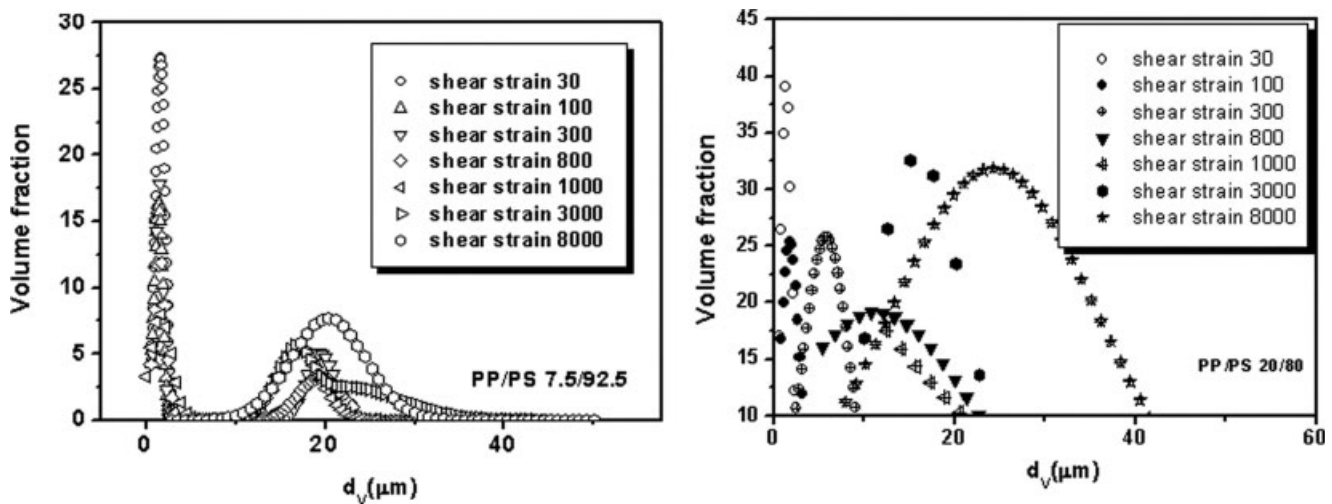


Figure 5 Shear-strain dependence of distribution of d_v .

was not found when concentration of PP exceeds 10%. Possible explanations for this result are given below. The first explanation is that the particle size at the beginning of coalescence is larger than d_{crit} . If so, the exponential relation might be observed by decreasing the initial particle size below d_{crit} and this is being studied recently in our laboratory. Another explanation is that eqs. (4)–(5) is not absolutely valid to describe quantitatively the initial stage coalescence in non-Newtonian PP/PS blends, after all, this model is originally established just for Newtonian fluid.

The size distribution is shown in Figure 5. From the very beginning, one can observe a very narrow particle size distribution shifting toward higher value of particle size with progressing time, and at the same time, the distribution width becomes more and more broader. In our previous work,²³ we used a log-normal distribution model to characterize the size distribution during the mixing process controlled by breakup mechanism. However, this distribution model is not appropriate to describe the size distribution during coalescence especially the late stage. For this reason, the Gaussian model²⁴ that is proved to be effective to quantify the size distribution during coalescence is used in this work and the evolution of the Gauss size distribution for PP/PS blends with different compositions is represented in Figure 5. As can be seen, while the peak width at half maximum becomes broader, a bimodal distribution appears between strain of 30–3000 when the concentration of minor phase is smaller (e.g., 7.5% in this work), the appearance of this interesting distribution can be ascribed to the asynchronous particles growth: at the very beginning of coalescence, some small particle collide and coalesce into big ones, leaving a number of small particles without coalescence. Further, since the coalescence efficiency decreases with increasing the difference in particle sizes, these after-formed big particles may not coalesce with those small ones, making those

remainder small particles stable for long times. Accordingly, a peak at smaller particles size is held on. However, in respect that the coalescence efficiency decreases with growth of particles, the coalescence between these big particles becomes more and more slower so that the late process becomes dominated by coalescence between smaller particles. As a result, the peak at lower particle size gradually disappears and a Gauss distribution appears again.

Figure 6 shows the variation of polydispersity (d_v/d_n) as a function of shear strain. d_v/d_n increases initially and reaches a maximum at strain between 3000 and 8000, and then it decreases monotonously. Since d_v reflects the coalescence between large particles while d_n shows that between smaller particles, the change of d_v/d_n indicates again that the early stage of coalescence is mainly controlled by coalescence between large particles and dominated by that between smaller ones later.

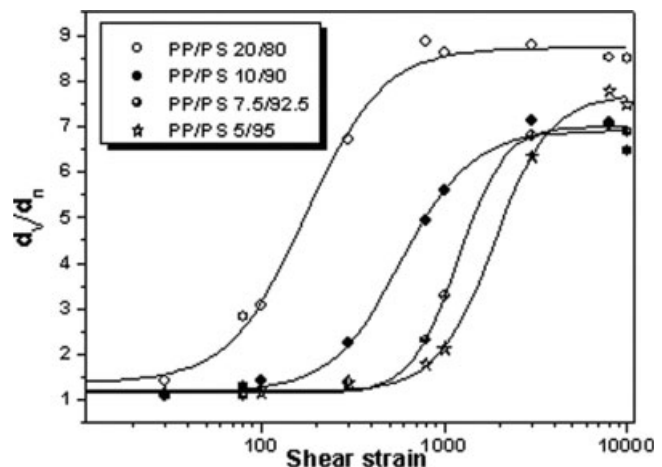


Figure 6 Variation of distribution dispersity of d as a function of shearing strain.

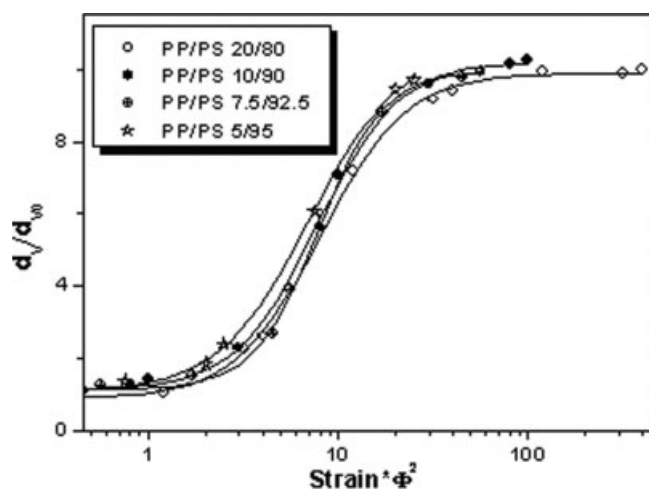


Figure 7 Scaling behavior during coalescence.

Besides the above-mentioned description of the shear-induced morphology development during coalescence, the scaling law was examined to study the coalescence mechanism. Scaling behavior has been studied before. For mixtures of Newtonian fluid, Vinckier et al.¹⁵ proposed a phenomenological model to describe the evolution of shape and size of interface in flow field. This model was later proved to be valid in the case of blends of viscoelastic polymers with different viscosity. Considering that the interfacial size is inversely proportional to the particle size, this model can be written in terms of particle size as:

$$\frac{d}{d_i} = f\left(\dot{\gamma}t, \frac{\dot{\gamma}}{\dot{\gamma}_i}\right) \quad (6)$$

where d_i is the initial particle size generated by particle breakup at higher shear rate $\dot{\gamma}_i$. It should be noted that eq. (6) is only valid for a certain composition of blend, and consequently, when the composition is an alterable parameter, this model should be amended to show the influence of composition on the scaling law. The composition influence on scaling law has been discussed by Rusu and Disdier.²⁵ According to them, eq. (6) can be changed to

$$\frac{d}{d_i} = f\left(\phi^2 \dot{\gamma}t, \frac{\dot{\gamma}}{\dot{\gamma}_i}\right) \quad (7)$$

Plotting data as suggested by eq. (7) (Fig. 7), one can see that curves with different compositions superpose with each other to form a master curve, confirming the scaling behavior during coalescence.

CONCLUSIONS

In this article, the shear-induced coalescence of particles in PP/PS blends with different compositions was investigated. The results show that the most increase in particle size occurs shortly after the beginning of the coalescence, which can be ascribed to the relatively higher coalescence efficiency during this period. Further increase in coalescence time has no significant effect on increasing particle size because of the drainage of matrix film between approaching particles, and consequently, the lower coalescence efficiency. Since the relatively smaller capillary number, the shear force is not strong enough to induce particle deformation. Thus, the particle remains spherical during the whole process. The results also show that the size distribution, which becomes more and more broader, can be better fitted by Gaussian distribution function except when the distribution curve shows a bimodal appearance. This interesting bimodal distribution can be ascribed to asynchronous particle growth and the longer life of small particles. The results also show that the coalescence process can be described by scaling law.

References

1. Taylor, G.I. Proc R Soc London Ser A 1934, 146, 501.
2. Torza, S.; Cox, R. G.; Mason, S. G. J Colloid Interface Sci 1972, 28, 395.
3. Wu, S. Polym Eng Sci 1987, 27, 335.
4. Grace, H. P. Chem Eng Commun 1982, 14, 225.
5. De Bruijin, R. A. Ph.D. Thesis, Eindhoven University of Technology, Eindhoven, 1989.
6. Jang, B. Z.; Uhlmann, D. R.; Sande, J. B. V. Rubber Chem Technol 1984, 57, 291.
7. Thomas, S.; Prud'homme, R. E. Polymer 1992, 33, 4260.
8. Park, D. W.; Roe, R. J. Macromolecules 1991, 24, 5324.
9. Favis, B. D.; Chalifoux, J. P. Polymer 1988, 29, 1761.
10. Datta, S.; Lohse, D. J. Macromolecules 1993, 26, 2064.
11. Sundararaj, U.; Macosko, C. W. Macromolecules 1995, 28, 2647.
12. Smoluchowski, V. Phys Chem 1917, 92, 129.
13. Zeichner, G. R.; Schowalter, W. R. AIChE J 1977, 23, 243.
14. Chester, A. K. Trans IChemE 1991, 69, 259.
15. Vinckier, I.; Moldenaers, P.; Terracciano, A. M.; Grizzuti, N. AIChE J 1998, 44, 951.
16. Rusu, D.; Peuvrel-Disdier, E. J Rheol 1999, 43, 1391.
17. Borschig, C.; Fries, B.; Gronski, W.; Weis, C.; Friedrich, C. Polymer 2000, 41, 3029.
18. Taylor, G. I. Proc R Soc London Ser A 1932, 38, 41.
19. Cox, R. G. J Fluid Mech 1969, 37, 601.
20. Swift, D. L.; Friedlander, S. K. J Colloid Sci 1964, 19, 621.
21. Wang, H.; Zinchenko, A. Z.; Davis, R. H. J Fluid Mech 1994, 265, 161.
22. Lyu, S.-P.; Bates, F. S.; Macosko, C. W. AIChE J 2002, 48, 7.
23. Li, Y.-Y.; Han, Y.-P.; Sheng, J. J Macrol Sci Phys 2004, 43, 1175.
24. Ziegler, V. E.; Wolf, B. A. Polymer 2005, 46, 9265.
25. Rusu, D.; Disdier, E. P. J Rheol 1999, 43, 1391.